Article

Hemicryptophanes with Improved Fluorescent Properties for the Selective Recognition of Acetylcholine over Choline

Augustin Long, Elise Antonetti, Alberto Insuasty, Sandra Pinet, Isabelle Gosse, Vincent Robert, Jean-Pierre Dutasta, and Alexandre Martinez

J. Org. Chem., **Just Accepted Manuscript** • DOI: 10.1021/acs.joc.0c00217 • Publication Date (Web): 06 Apr 2020

Hemicryptophanes with Improved Fluorescent Properties for the Selective Recognition of Acetylcholine over Choline

Augustin Long,[†] Elise Antonetti,[†] Alberto Insuasty,[†] Sandra Pinet,[§] Isabelle Gosse,[§] Vincent Robert,[⊥] Jean-Pierre Dutasta,[‡] and Alexandre Martinez*[†]

[†] Aix-Marseille Univ., CNRS, Centrale Marseille, iSm2, UMR 7113, 13397, Marseille, France

[§] ISM, UMR 5255 CNRS, Bordeaux INP and Univ. Bordeaux, 351 cours de la Libération, F-33400 Talence, France.

[⊥] Laboratoire de Chimie Quantique Institut de Chimie, UMR CNRS 7177, Université de Strasbourg, 4, rue Blaise Pascal, F-67070 Strasbourg, France.

‡ Laboratoire de Chimie, Ecole Normale Supérieure de Lyon, CNRS, UCBL, 46 allée d'Italie, F-69364 Lyon, France

Supporting Information Placeholder

ABSTRACT: The synthesis of two new fluorescent hemicryptophanes is reported. They were found to be efficient and selective receptors for acetylcholine over choline. When compared to other hemicryptophane hosts previously reported for the selective recognition of acetylcholine, they display improved fluorescent properties: their maximum emission wavelengths are red shifted and the quantum yields are higher. NMR titration experiments and DFT calculations support the results obtained from fluorescence spectroscopy and give insights into the interactions involved in the host/guest complexes and into the selectivity for acetylcholine over choline.

INTRODUCTION

Acetylcholine (ACh) is a neurotransmitter that plays a crucial role in both the peripheral and central nervous systems. For instance, ACh is involved in learning and memory processes or in the transmission and regulation of the nervous impulse in the synaptic key.[1-4] Therefore, the development of synthetic receptors for ACh has arouse a considerable interest.[5-13] In particular, fluorescent supramolecular probes have been designed to detect ACh as they allow for high sensitivity, technical simplicity and fast response time, and are thus convenient for optical imaging and analytical sensing.[14-15] Although several fluorescent host compounds able to detect ACh have been reported,[16-21] only few display ACh/Choline (Ch) selectivity in favor of ACh.[22-30] Recently, we reported the synthesis of the fluorescent hemicryptophane **1**, which is able to recognize ACh with a selectivity K_{ACh}/K_{Ch} of 4.1 (Figure 1).[31,32] However, this host suffers from modest fluorescent properties due to the naphthalene units included in the linkers of the cage compound, which lead to a modest quantum yield (1.8%) and wavelength emission at 326 nm. We thus decided to add additional conjugated units in order to improve the fluorescent properties of the host without altering the size and shape of the cavity, aiming at preserving a good ACh>Ch selectivity. Herein we report on the synthesis of the new hemicryptophanes **2** and **3** bearing fluorescent linkers (Figure 1). The fluorescent properties have been improved when compared to our previously reported cage **1**, while the ACh/Ch selectivity is retained.

Figure 1. Structures of the hemicryptophane hosts (**1**-**3**) and the guests used in this study.

RESULTS AND DISCUSSION

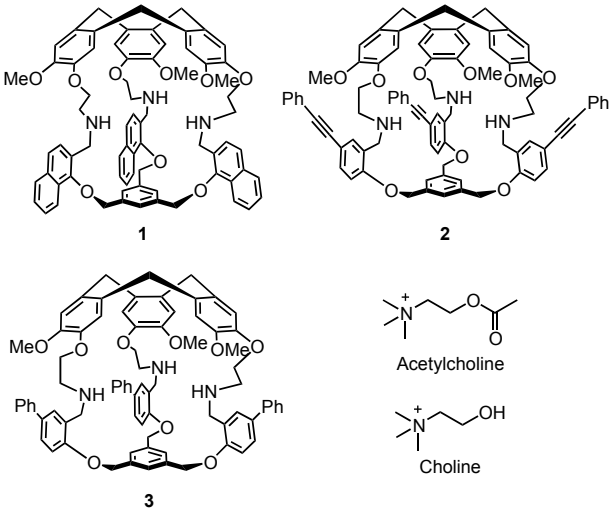

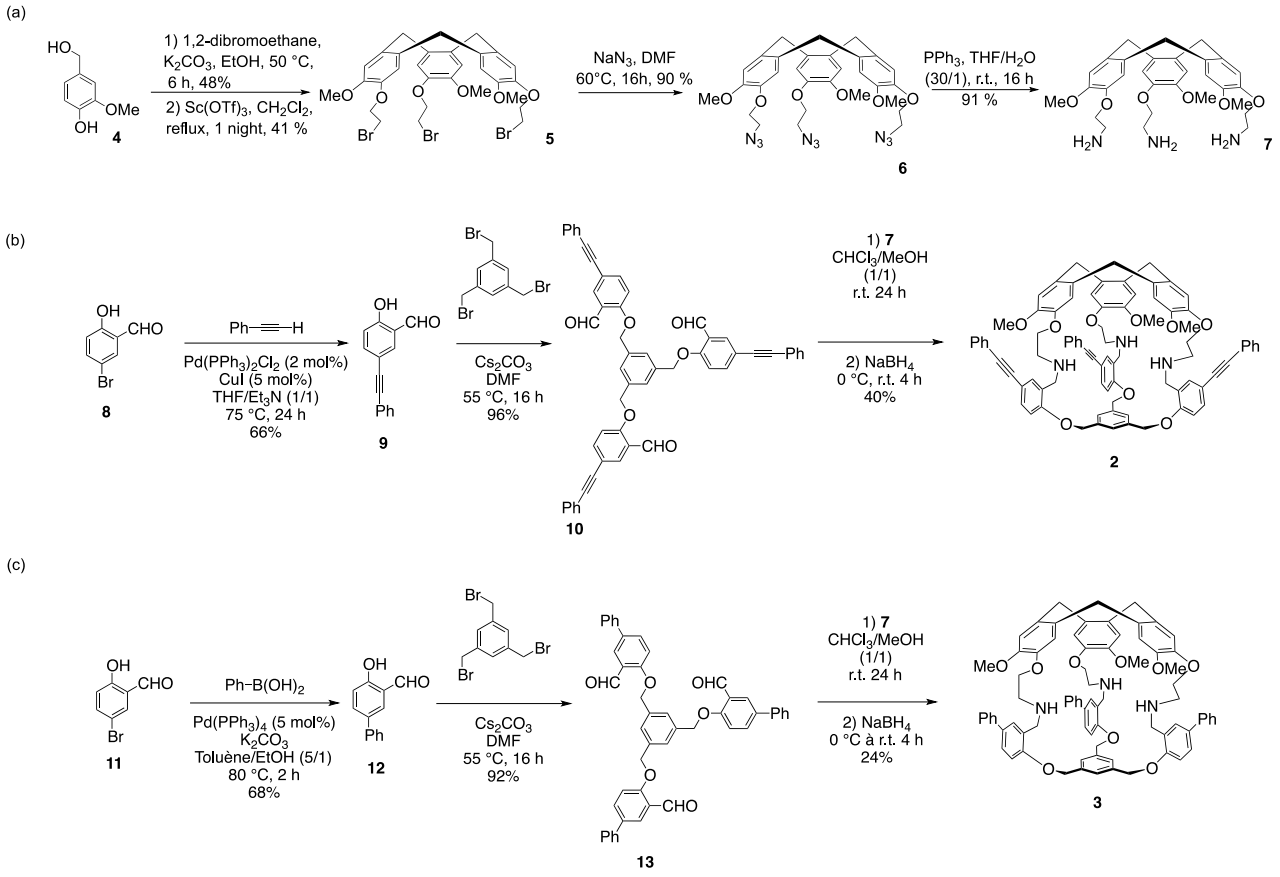

Scheme 1. Synthesis of key intermediate 7 (a) and of hemicryptophanes 2 (b) and 3 (c).

Fluorescent hemicryptophanes **2** and **3** have been obtained following the synthetic pathways shown in Scheme 1. Firstly, the tris(ethanamine)-cyclotriveratrylene derivative **7** (CTV-NH_2) is synthesized according to our previously reported 4-steps procedure: the reaction of vanillyl alcohol with dibromoethane in EtOH followed by triple Friedel-Crafts reaction in MeCN with $Sc(OTf)_3$ as catalyst affords CTV-Br **5** in 20 % yield.[33] The three bromine atoms are then substituted by azide functions, and a subsequent Staudinger's reaction gives CTV-NH_2 **7** with 15% overall yield.[34] This key intermediate **7** was used for the synthesis of cages **2** and **3**. Secondly, 5-bromo-2-hydroxybenzaldehyde reacts under classical Sonogashira coupling conditions or Suzuki coupling conditions to afford **9** and **12** in 66% and 68% yields, respectively. Then, nucleophilic substitutions of the phenol unit of **9** and **12** on 1,3,5-tribromomethyl-benzene, using Cs_2CO_3 as a base, give the C_3-symmetrical trialdehydes **10** and **13** in 96% and 92 % yields, respectively. Finally, reductive aminations between CTV-NH_2 **7** and trialdehydes **10** and **13** afford cages **2** and **3** in 40% and 24% yields respectively.

^{1}H NMR spectra (Figure 2) show that both cages **2** and **3** exhibit the C_3-symmetry usually observed for hemicryptophane hosts in solution. Both present characteristic signals of cages including a CTV moiety: two doublets

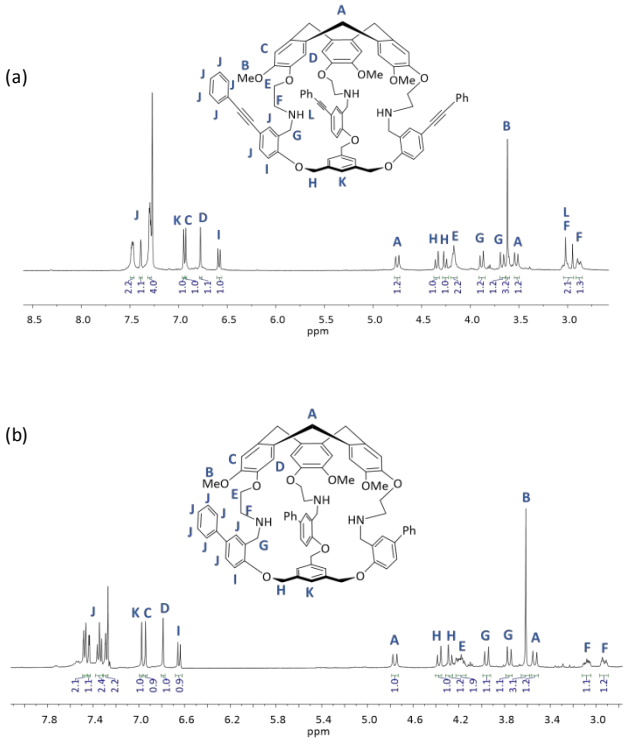

Figure 2. ^{1}H NMR spectra (400 MHz, $CDCl_3$, 298 K) of hemicryptophanes **2** (a) and **3** (b).

for the $ArCH_2$ methylene bridges (**A**) around 4.8 and 3.5 ppm, the two singlets around 6.95 and 6.8 ppm for the aromatic protons (**C**, **D**) and a singlet near 3.6 ppm for the methoxy groups (**B**). The aromatic protons (**K**) and the diastereotopic aliphatic protons (**H**) of the lower part appear as a singlet at 7.0 ppm and an AB quartet around 4.3 ppm, respectively. The diastereotopic protons **G** of the linkers give two AB doublets near 3.7 and 3.9 ppm, whereas the protons **F** and **E** give slightly more complicated pattern around 3.0 and 4.2 ppm respectively. The aromatic protons **J** of the linkers are also observed as multiplets between 7.2 and 7.6 ppm, while the doublet around 6.6 ppm is characteristic of the aromatic proton **I**.

The absorption and emission properties of compounds **2** and **3** in DMSO containing 2% of water are shown in Figure 3. The maximum emission wavelengths of **2** and **3** are in both cases red shifted compared to host **1**: from 326 nm ($\varepsilon = 2.0 \times 10^4$ M^{-1} cm^{-1}) for host **1** to 352 nm ($\varepsilon = 9.4 \times 10^4$ M^{-1} cm^{-1}) and 334 nm ($\varepsilon = 5.1 \times 10^4$ M^{-1} cm^{-1}) for hosts **2** and **3**, respectively (Table 1). The fluorescent quantum yields Φ are also improved when compared to host **1**: from 1.8% for cage **1** to 5.4% and 7.5% for hosts **2** and **3**, respectively (Table 1).[34]

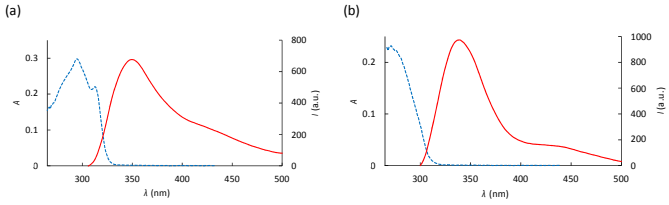

Figure 3. Absorption spectra (in blue) and emission spectra (in red, λ_{exc} = 290 nm): (a) hemicryptophane **2** (3.2 µM) and (b) hemicryptophane **3** (4.7 µM) in solution in DMSO + 2% H_2O at 298 K.

Table 1. Spectroscopic data of cages 1, 2 and 3 in DMSO with 2% of water at 298 K.

Host	λ_{abs}^{max} (nm)	ε ($L.mol^{-1}.cm^{-1}$)	λ_{em}^{max} (nm)	Δλ (nm)	φ_f
1	288	2.0×10^4	326	38	1.8%
2	294	9.4×10^4	352	58	5.4%
3	274	5.1×10^4	334	60	7.5%

We then studied the recognition of ACh and Ch by these two new hosts **2** and **3**. Additions of a solution of ACh or Ch in DMSO + 2% H_2O to hosts **2** and **3** induce changes in fluorescence emission of the cages (Figure 4 for ACh and Figures S24 and S25 for Ch). However, the fluorescence response of these compounds strongly differs upon addition of the neurotransmitter guests. Cage **3** shows the same behavior as that reported for cage **1**: an increase of the fluorescence intensity is observed, whereas cage **2** displays a decrease of the fluorescence intensity upon progressive addition of guest solutions. The expected higher rigidity of cage **2** might account for this opposite behavior. Both hosts **2** and **3** exhibit binding constants for ACh and Ch in the same range of magnitude than those of cage **1** (typically in the range of 10^4 M^{-1}, see Table 2), highlighting that the introduction of fluorescent units in the linkers only slightly affects the binding properties of the host, probably because the size and shape of the cavity are similar in all cases. The ACh/Ch selectivity is also retained, with a K_{ACh}/K_{Ch} ratio of 2.8 and 4.4 for hosts **2** and **3** respectively.

Table 2. Binding constants Ka (M^{-1}) for the 1:1 complexes formed between the different hosts and guests.

Substrate	Host	K_a ($L.mol^{-1}$)[a]	K_{ACh}/K_{Ch}
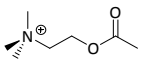 ACh	**1**	$2.4 \times 10^4 \pm 2.0\%$	-
	2	$1.2 \times 10^4 \pm 2.1\%$	-
	3	$4.4 \times 10^4 \pm 4.4\%$	-
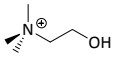 Ch	**1**	$5.9 \times 10^3 \pm 2.3\%$	4.1
	2	$4.3 \times 10^3 \pm 2.2\%$	2.8
	3	$1.0 \times 10^4 \pm 4.8\%$	4.4

[a] K_a was determined by fitting fluorescence titration curves (DMSO + 2% H_2O, 298 K) with Bindfit program.

^1H NMR titration experiments were also performed to give insight into these recognition processes. To a solution of hosts **2** or **3** in a $CDCl_3$/MeOH mixture (95/5), was added a concentrated solution of ACh or Ch in the same solvent mixture. Changes in the chemical shifts of both, the cages and the guests, were observed (Figures S30-S37), which is in agreement with the expected fast host-guest exchange on the NMR time scale that is usually observed with hemicryptophane hosts. One can see that, by increasing the ACh or Ch concentrations, both their $(CH_3)_3N$ and CH_2 protons are downfield shifted. At the beginning of the titration experiment the Ach or Ch guest is mostly encapsulated in the host and undergoes the shielding effect of the aromatic rings of hosts **2** and **3**, leading to the upfield chemical shifts observed for $N(CH_3)_3$ and CH_2 protons compared to that of the free guests in solution. The successive additions of Ach or Ch guest increase the percent of the free guests and results in an average chemical shift shifted towards that of the free guest, which explains the downfield shift observed for the protons' guest during the titration experiments. This is consistent with the encapsulation of the guests in the heart of the cavities. For both hosts **2** and **3**, the protons **A**, **H** and **J** exhibit well-defined and sharp signals and no overlapping with the signals of other protons occurs during the titration experiments. Therefore, the

variations of their chemical shifts against the guest/host ratio were plotted and the resulting titration curves were fitted with the Bindfit program, giving binding constants for ACh of 4.7×10^3 L.mol^{-1} and 6.2×10^3 L.mol^{-1} and for Ch of 6.49×10^2 L.mol^{-1} and 2.9×10^2 L.mol^{-1} for host **2** and **3** respectively.[35] The difference in the solvent as well as the change in the counterions used for NMR and fluorescent titration experiments could account for the difference of the binding constants measured by these two methods. Moreover, the changes in the chemical shifts during the NMR titration experiments are rather small, inducing higher errors in the determination of the Ka values. However, these NMR titration experiments nicely support the fluorescence ones, highlighting the remarkable ACh/Ch selectivity of this class of fluorescent hosts.

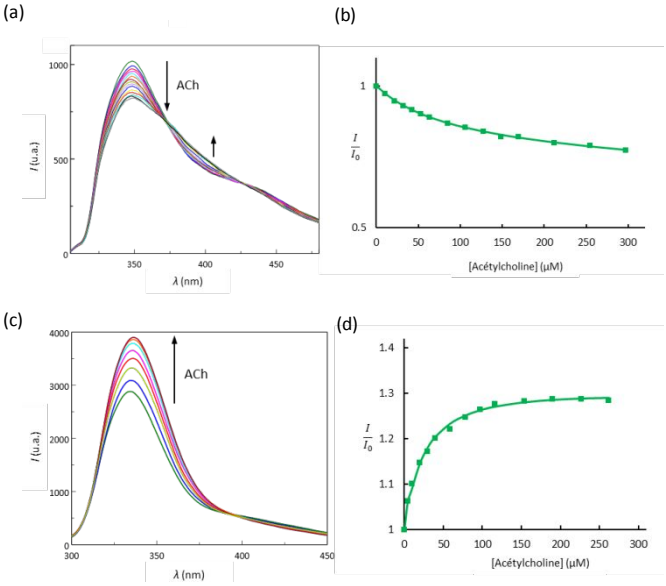

Figure 4. Fluorescent emission spectra at 298 K (λ_{exc} = 290 nm) in DMSO + 2% H_2O of a solution of (a) hemicryptophane **2** (5.0 µM) and (c) hemicryptophane **3** (5.0 µM) upon progressive additions of a solution of ACh (5.0 mM, counterion Cl^-). Evolution of the relative fluorescence intensity as a function of the concentration of added ACh: (b) at 348 nm for host **2**, and (d) at 338 nm for host **3**. Curves were fitted with the Bindfit program (lines).[35]

Then, DFT calculations were performed to grasp the interactions involved in these recognition processes. The optimized structures (Figure 5) show a partial encapsulation of ACh in receptors 2 and 3. The ammonium unit is located below the CTV moiety, in agreement with the NMR titration experiments where shielding of the $(CH_3)_3N$ protons was observed in the presence of the cages. The ammonium unit interacts with both the aromatics of the CTV and that of the south part by CH-π interactions (C-H…C_{ar} distances between 2.35 and 2.62 Å). Furthermore, hydrogen bonding between (i) the oxygen of the C=O carbonyl of ACh and the Ar-CH_2 and N-H protons of the receptors and (ii) the CH_2 and C(O)-CH_3 protons of ACh and the oxygen atoms of the CTV unit can be observed (distances between 2.2 and 2.5 Å). Thus, these DFT calculations give insight into the origin of the ACh/Ch selectivity: as Ch lacks the key ester function, these interactions described above are not possible with this guest, leading to a decrease of its affinity for the cavity of the hemicryptophanes, when compared to ACh.

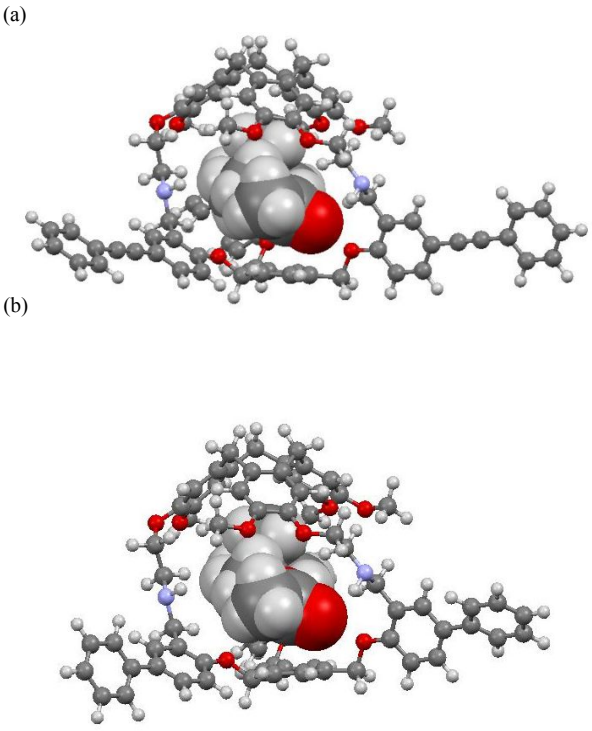

Figure 5. DFT optimized structures of the encapsulated acetylcholine guest within the cavity of the fluorescent hemicryptophanes **2** (a) and **3** (b).

CONCLUSION

In summary, the synthesis of two new hemicryptophane cages **2** and **3** with improved fluorescent properties, when compared to previously reported host **1**, has been described. These cages turn out to be efficient receptors for neurotransmitter ACh displaying a marked selectivity for ACh over Ch. Whereas cage **3** behaves as a turn ON receptor of ACh, a decrease of fluorescence is observed when ACh is added to hemicryptophane **2**. Insights into the structure of the host/guest complexes have been obtained from NMR titration experiments and DFT calculations. Studies for longer-wavelength fluorescence detection, and detection in water, using hemicryptophanes, are underway.

EXPERIMENTAL SECTION

General. Commercial grade solvents and starting material were used without additional purification. Chromatography and TLC were carry out with Merck 60 A (0.040 - 0.063 mm) silica gel and Merck silica gel 60 F_{254} plates respectively. A Büchi Melting Point B-545 was used for the determination of the melting points. A Bruker Alpha Platinum ATR allowed for the recording of the IR spectra. ^{1}H NMR and ^{13}C NMR were carry out at 298 K on either a Bruker Avance III HD 400 MHz a Bruker Avance III HD or 300 MHz spectrometer. The protonated residual solvent signal was used as reference for reporting the ^{1}H NMR and ^{13}C NMR chemical shifts δ. HRMS were performed on a SYNAPT G2 HDMS (Waters) mass spectrometer with API and spectra were obtained with TOF analysis using two internal standards. UV spectra were carry out on a Agilent Cary 60 UV-Vis spectrophotometer and fluorescence spectra on a Jasco FP-8600 spectrofluorometer. CTV-Br derivative **5,** CTV-NH_2 **7** and hemicryptophane **1** were synthesized according to the previously reported procedure.[32-34]

Synthesis of compound 9. 5-Bromo-2-hydroxy-benzaldehyde **8** (1.61 g, 8.00 mmol), CuI (79 mg, 0.41 mmol) and $Pd(PPh_3)_2Cl_2$ (282 mg, 0.19 mmol) were added in a 100 mL round-bottom flask under argon atmosphere. A 1/1 mixture of THF and Et_3N (35 mL) were added. Ethynylbenzene (1.75 mL, 15.9 mmol) was added and the mixture was stirred under argon at 75 °C (oil bath) during 24 h. The mixture was cooled to r.t. and diluted with Et_2O (50 mL) and water (50 mL). The aqueous layer was acidified with 2M HCl solution (40 mL). The layers were separated and the aqueous phase was extracted with Et_2O (50 mL). Organic layers were combined, washed with brine (60 mL) and dried over $MgSO_4$, filtered and concentrated under vacuum. The crude was purified by silica gel column chromatography with a gradient of petroleum ether and EtOAc (from 19/1 to 17/3) as eluent to afford **9** as a white powder (1.18 g, 66%). Rf = 0.33 (PE/EtOAc: 95/5); ^{1}H NMR (400 MHz, $CDCl_3$, 298 K) δ 11.14 (s, 1H), 9.92 (s, 1H), 7.79 (d, J = 2.0 Hz, 1H), 7.70 (dd, J = 8.6; 2.0 Hz, 1H), 7.57–7.52 (m, 2H), 7.41–7.36 (m, 3H), 7.02 (d, J = 8.6 Hz, 1H); ^{13}C{^{1}H} NMR (100 MHz, $CDCl_3$, 298 K) δ 196.1, 161.4, 139.8, 136.9, 131.5, 128.4, 122.9, 120.5, 118.1, 115.3, 88.9, 87.5; IR ν = 3054, 2924, 2856, 1656, 1594, 1494, 1142, 1123 cm^{-1}; HRMS (ESI-TOF) m/z: [M-H]$^-$ Calcd for $C_{15}H_9O_2$ 221.0608; Found 221.0608; m.p. = 82 – 83 °C.

Synthesis of compound 10. In a 100 mL round-bottom flask were dissolved 1,3,5-tris(bromomethyl)benzene **11** (201 mg, 0.563 mmol) and compound **9** (418 mg, 1.88 mmol) in DMF (30 mL). Cs_2CO_3 (770 mg, 2.36 mmol) was added and the mixture was stirred at 55 °C (oil bath) for 16 h. The mixture was diluted with EtOAc (100 mL), washed with a 10% NaOH solution (4 x 50 mL), brine (2 x 40 mL) and dried over $MgSO_4$. The solvent was removed under reduce pressure to give **10** a slightly orange solid (422 mg, 96%). R_f = 0.13 (PE/CH_2Cl_2: 20/80); ^{1}H NMR (400 MHz, $CDCl_3$, 298 K) δ 10.52 (s, 1H), 8.05 (d, J = 2.2 Hz, 1H), 7.71 (dd, J = 8.6; 2.2 Hz, 1H), 7.56–7.50 (m, 3H), 7.36–7.33 (m, 3H), 7.05 (d, J = 8.7 Hz, 1H), 5.30 (s, 2H); ^{13}C{^{1}H} NMR (100 MHz, $CDCl_3$, 298 K) δ 188.6, 160.1, 138.6, 137.3, 132.4, 131.6, 128.4, 125.9, 125.2, 123.0, 116.8, 113.2, 89.5, 87.7, 70.2; IR ν = 2922, 2854, 1682, 1592, 1496, 1268, 1220 cm^{-1}; HRMS (ESI-TOF) *m/z*: $[M+NH_4]^+$ calcd for $C_{54}H_{40}NO_6$ 798.2850; Found 798.2855; m.p. = 87 – 88 °C.

Synthesis of Compound 12. In a 100 mL round-bottom flask, 5-bromo-2-hydroxybenzaldehyde **8** (1.01 g, 5.02 mmol) was dissolved in toluene (25 mL) and EtOH (5 mL) under argon atmosphere. Phenylboronic acid (1.25 g, 10.2 mmol), K_2CO_3 (1.75 g, 12.5 mmol) and $Pd(PPh_3)_4$ (302 mg, 0.26 mmol) were added successively under stirring. The reaction mixture was heated at 80 °C (oil bath) for 2 h. Solvents were removed under reduced pressure and the reaction mixture was extracted with EtOAc (2 x 30 mL) and washed with a 1 M HCl solution (2 x 30 mL). Organic layers were combined, washed, dried over $MgSO_4$ and the solvent was removed. The crude was purified by silica gel column chromatography with petroleum ether and EtOAc (98/2) as eluent to afford **12** as a yellow powder (582 mg, 68%). R_f = 0.41 (PE/EtOAc: 95/5); ^{1}H NMR (300 MHz, $CDCl_3$, 298 K) δ 11.00 (s, 1H), 9.98 (s, 1H), 7.80–7.75 (m, 2H), 7.59–7.53 (m, 2H), 7.49–7.42 (m, 2H), 7.40–7.33 (m, 1H), 7.08 (d, J = 8.7 Hz, 1H); ^{13}C{^{1}H} NMR (75 MHz, $CDCl_3$, 298 K) δ 196.6, 161.0, 139.4, 135.7, 133.4, 131.9, 129.0, 128.8, 127.4, 126.8, 126.6, 120.8, 118.2; IR ν = 3070, 2932, 2876, 1660, 1591, 1491 cm^{-1}; HRMS (ESI-TOF) *m/z*: [*M*-H]$^-$ calcd for $C_{13}H_9O_2$ 197.0908; Found 197.0907; m.p. = 93 – 94 °C.

Synthesis of compound 13. Compound **12** (274 mg, 1.38 mmol) and 1,3,5-tris(bromomethyl)benzene **11** (153 mg, 0.43 mmol) were dissolved in DMF (40 mL). Cs_2CO_3 (612 mg, 1.88 mmol) was added and the mixture was stirred at 55 °C (oil bath) for 16 h. The solid obtained was filtered on a frit and washed with cold ethanol and cold water to yield **13** as a slightly yellow powder (287 mg, 92%). R_f = 0.16 (PE/CH_2Cl_2: 20/80); ^{1}H NMR (300 MHz, $CDCl_3$, 298 K) δ 10.60 (s, 1H), 8.11 (d, J = 2.5 Hz, 1H), 7.78 (dd, J = 8.6; 2.5 Hz, 1H), 7.59–7.54 (m, 3H), 7.46–7.32 (m, 3H), 7.12 (d, J = 8.7 Hz, 1H), 5.33 (s, 2H); ^{13}C{^{1}H} NMR (75 MHz, $CDCl_3$, 298 K) δ 189.4, 160.0, 139.3, 137.6, 134.5, 134.3, 128.9, 127.4, 127.2, 126.7, 125.8, 125.4, 113.5, 70.3; IR ν = 2932, 2857, 1688, 1595, 1491, 1260 cm^{-1}; HRMS (ESI-TOF) *m/z*: [*M*+NH_4]$^+$ Calcd for $C_{48}H_{40}NO_6$ 726.2850; Found 726.2852; m.p. = 114 – 116 °C.

Synthesis of hemicryptophane 2.In a 500 mL round-bottom flask was dissolved CTV **7** (128 mg, 0.238 mmol) in a 1/1 mixture of $CHCl_3$/MeOH (120 mL). A solution of **10** (169 mg, 0.216 mmol) in the same mixture of solvent (100 mL) was added dropwise under stirring at r.t. and the reaction mixture was stirred at r.t.

for 24 h. It was cooled to 0 °C and $NaBH_4$ (290 mg, 7.67 mmol) was added portionwise. The mixture was stirred at r.t. for 4 h and solvents were evaporated. The crude residue was dissolved in $CHCl_3$ (50 mL) and washed with a 10% NaOH solution (50 mL). Aqueous phase was extracted with $CHCl_3$ (50 mL) and combined organic layers were washed with a 10% NaOH solution (3 x 40 mL), dried over $MgSO_4$ and filtered. Organic solvent was removed under reduced pressure to afford a yellowish solid purified by silica gel column chromatography with $CHCl_3$/MeOH/Et_3N as eluent (gradient from 97/1/2 to 93/6/2). Hemicryptophane **2** was obtained as a white solid (110 mg, 40%). R_f = 0.27 ($CHCl_3$/MeOH/Et_3N: 95/3/2); λ_{max} = 284 nm (DMSO + 2% H_2O, ε = 94 000 L.mol^{-1}.cm^{-1}); ^{1}H NMR (400 MHz, $CDCl_3$, 298 K) δ 7.49–7.46 (m, 2H), 7.40–7.37 (m, 1H), 7.31– 7.28 (m, 4H), 6.95 (s, 1H), 6.93 (s, 1H), 6.78 (s, 1H), 6.58 (d, J = 8.5 Hz, 1H), 4.75 (d, J = 13.6 Hz, 1H), 4.35 (d, J = 11.9 Hz, 1H), 4.26 (d, J = 12.0 Hz, 1H), 4.20–4.13 (m, 2H), 3.88 (d, J = 13.5 Hz, 1H), 3.67 (d, J = 13.5 Hz, 1H), 3.62 (s, 3H), 3.53 (d, J = 13.9 Hz, 1H), 3.05–2.94 (m, 2H), 2.92–2.85 (m, 1H); ^{13}C{^{1}H} NMR (100 MHz, $CDCl_3$, 298 K) δ 156.47, 148.60, 146.87, 137.02, 133.52, 132.94, 131.88, 131.46, 128.27, 127.88, 126.97, 123.57, 116.39, 115.28, 113.47, 111.87, 89.28, 88.18, 69.17, 69.09, 55.84, 49.11, 47.78, 36.41; IR ν = 3332, 2924, 1606, 1507, 1260, 1240, 1142 cm^{-1}; HRMS (ESI-TOF) *m/z*: [*M*+2H]$^{2+}$ Calcd for $C_{84}H_{77}N_3O_9$ 635.7824; Found 635.7819; m.p. = 169 – 171 °C.

Synthesis of hemicryptophane 3. In a 250 mL round-bottom flask was added CTV **7** (99 mg, 0.184 mmol) dissolved in a 1/1 mixture of $CHCl_3$/MeOH (120 mL). A solution of **13** (117 mg, 0.166 mmol) in the same mixture of solvent (120 mL) was added dropwise under stirring at r.t. and the reaction mixture was stirred at r.t. overnight. $NaBH_4$ (240 mg, 6.35 mmol) was added portionwise at 0 °C and the mixture was stirred at r.t. during 4 h. Solvents were evaporated, the crude residue was dissolved in $CHCl_3$ (30 mL) and washed with a 10% NaOH solution (30 mL). Aqueous phase was extracted twice with $CHCl_3$ (2 x 30 mL) and combined organic layers were washed with a 10% NaOH solution (3 x 25 mL) and dried over $MgSO_4$. Organic solvent was removed under reduced pressure to afford a white solid purified by silica gel column chromatography ($CHCl_3$/MeOH/Et_3N, gradient from 97/1/2 to 90/8/2). Hemicryptophane **3** was obtained as a white solid (48 mg, 24%). R_f = 0.31 ($CHCl_3$/MeOH/Et_3N: 95/3/2); λ_{max} = 274 nm (DMSO + 2% H_2O, ε = 51 000 L.mol^{-1}.cm^{-1}); ^{1}H NMR (400 MHz, $CDCl_3$, 298 K) δ 7.50–7.43 (m, 3H), 7.39–7.33 (m, 2H), 7.33–7.28 (m, 2H), 6.97 (s, 1H), 6.95 (s, 1H), 6.79 (s, 1H), 6.65 (d, J = 8.5 Hz, 1H), 4.76 (d, J = 13.7 Hz, 1H), 4.36 (d, J = 12.1 Hz, 1H), 4.30–4.14 (m, 3H), 3.97 (d, J = 13.3 Hz, 1H), 3.78 (d, J = 13.2 Hz, 1H), 3.62 (s, 3H), 3.54 (d, J = 13.6 Hz, 1H), 3.14–3.05 (m, 1H), 2.98–2.90 (m, 1H), 2.20 (s, 1H); ^{13}C{^{1}H} NMR (100 MHz, $CDCl_3$, 298 K) δ 155.93, 148.67, 146.87, 140.59, 137.28, 133.50, 133.02, 131.87, 128.97, 128.69, 126.89, 126.73, 126.65, 126.59, 116.54, 113.46, 112.21, 69.11, 69.03, 55.83, 49.51, 47.90, 36.44; IR ν = 3348, 2912, 1613, 1511, 1413, 1248, 1206, 1108 cm^{-1}; HRMS (ESI-TOF) *m/z*: [*M*+2H]$^{2+}$ Calcd for $C_{78}H_{77}N_3O_9$ 599.7824; Found 599.7823; m.p. = 187-189 °C.

Photophysic studies

The absorption spectrum of a solution in DMSO + 2% H_2O of each hemicryptophane was recorded between 265 nm and 500 nm using a quartz cuvette (1 cm x 1 cm x 4.5 cm).

The emission spectrum was recorded between 300 nm and 550 nm. Emission spectra of 4 solutions of each hemicryptophane in DMSO containing 2% H_2O, with absorbance lower than 0.1, were recorded, and the average quantum yield was calculated with quinine bisulfate in H_2SO_4 (0.5 M). All these solutions afforded the same results. Spectra were recorded on a Jasco FP-8600 spectrofluorometer equipped with a JASCO Peltier cell holder ETC-815 to maintain the temperature at 25.0 ± 0.2°C.

Fluorescence titrations. A solution of each hemicryptophane (2.5 mL, 5.0 μM) in DMSO + 2% H_2O was taken into the quartz cuvette, and then certain equivalents of a concentrated guest solution (5.0 mM) in the same solvents were added stepwise with a microsyringe. The final volume of the solution was almost unchanged (2.5 mL) since very small volume of guest solution was added. The solution was mixed and incubated for 30 s before irradiation at 290 nm at 25 °C. The corresponding emission values during titration were then recorded.

NMR titrations. A solution of hemicryptophane host **2** or **3** (1.0×10^{-3} M in $CDCl_3$/CD_3OD 95/5, 500 μL) was titrated in NMR tubes with aliquots of a concentrated solution (5.0×10^{-3} M in the same solvent) of picrate salts of neurotransmitters. The shifts Δδ of the host's protons signals at 7.61 and 7.55 ppm were measured after each addition and plotted as a function of the substrate/receptor ratio ([S]/[R]). Association constant K_a was obtained by nonlinear least-squares fitting of these plots using Bindfit program from Thordarson's group.[35]

Computational method. In order to access geometrical information upon the host–guest species, full geometry optimizations were performed using restricted Density Functional Theory (DFT) calculations. A combination of BP86 functional and an all electron 6-31G* basis set including polarization functions has proven to be very satisfactory for similar issues.[36] However, we checked using the hybrid B3LYP functional that our results do not suffer from the arbitrariness of the exchange correlation functional. All calculations were carried out using the Gaussian 03 suite of program.[37]

ASSOCIATED CONTENT

Supporting information

The Supporting Information is available free of charge on the ACS Publications website.
^{1}H and ^{13}C NMR, mass and UV spectra, titration experiments and cartesian coordiantes (PDF).

AUTHOR INFORMATION

Corresponding Author

* E-mail: alexandre.martinez@centrale-marseille.fr

Notes

The authors declare no competing financial interest.

REFERENCES

(1) Descarries, L.; Umbriaco, D. Ultrastructural basis of monoamine and acetylcholine function in CNS. *Semin. Neurosci.* **1995**, *7*, 309–318.

2 Tsai, T.-H. Separation methods used in the determination of choline and acetylcholine. *J. Chromatogr. B. Biomed. Sci. Appl.* **2000**, *747*, 111–122.

3 Kandel, E. R.; Schwartz J. H.; Jessell, T. M. Principles of Neural Science, MacGraw Hill, United States, 4th edn., **2000**.

4 Cooper, J. R.; Bloom F. E.; Roth, R. H. The biochemical basis of neuropharmacology, Oxford University Press, New York, **1991**.

5 Dhaenens, M.; Lacombe, L.; Lehn J.-M.; Vigneron, J.-P. Binding of acetylcholine and other molecular cations by a macrocyclic receptor molecule of speleand type. *J. Chem. Soc. Chem. Commun.* **1984**, 1097–1099.

6 Dougherty D. A.; Stauffer, D. A. Acetylcholine binding by a synthetic receptor: implications for biological recognition. *Science,* **1990**, *250*, 1558–1560.

7 Lehn, J.-M.; Meric, R.; Vigneron, J.-P.; Cesario, M.; Guilhem, J. ; Pascard, C.; Asfari Z.; Vicens, J. Binding of acetylcholine and other quaternary ammonium cations by sulfonated calixarenes. Crystal structure of a [choline-tetrasulfonated calix[4]arene] complex. *Supramol. Chem.* **1995**, *5*, 97–103.

8 Bartoli, S.; Roelens, S. Binding of Acetylcholine and Tetramethylammonium to a Cyclophane Receptor: Anion's Contribution to the Cation−π Interaction. *J. Am. Chem. Soc.* **2002**, *124*, 8307–8315.

9 Zelder, F. H.; Rebek, J. R. Jr Cavitand templated catalysis of acetylcholine. *Chem. Commun.* **2006**, 753–754.

10 Park, Y. S.; Kim, Y.; Paek, K. Park, Y. S.; Kim, Y.; Paek, K. *Org. Lett.* **2019**, *21*, 8300−8303.

11 Abdoul-Carime, H.; Harb, M. M.; Montano, C. G.; Teyssier, C.; Farizon, B.; Farizon, M.; Vachon, J.; Harthong, S.; Dutasta, J.-P.; Jeanneau E.; Märk, T. D. Selective host–guest chemistry investigated by mass spectrometry: Which of the two, choline or acetylcholine, is the preferred one by the 3iPO triphosphonate-cavitand ? *Chem. Phys. Lett.* **2012**, *533*, 82–86;

12 Jin, T. Near-Infrared Fluorescence Detection of Acetylcholine in Aqueous Solution Using a Complex of Rhodamine 800 and p-Sulfonato-calix[8]arene. *Sensors* **2010**, *10*, 2438–2449.

13 Ma, J.; Meng, Q.; Hu, X.; Li, B.; Ma, S.; Hu, B.; Li, J.; Jia X.; Li, C. Synthesis of a Water-Soluble Carboxylatobiphen[4]arene and Its Selective Complexation toward Acetylcholine. *Org. Lett*. **2016**, *18*, 5740–5743.

14 de Silva, A. P.; Gunaratne, H. Q. N.; Gunnlaugsson, T.; Huxley, A. J. M.; McCoy, C. P.; Rademacher J. T; Rice, T. E. Signaling Recognition Events with Fluorescent Sensors and Switches. *Chem. Rev*. **1997**, *97*, 1515–1566.

15 Pradhan, T.; Jung, H. S.; Jang, J. H.; Kim, T. W.; Kang C.; Kim, J. S. Chemical sensing of neurotransmitters. *Chem. Soc. Rev.* **2014**, *43*, 4684–4713.

16 Inouye, M.; Hashimoto K.; Isagawa, K. Nondestructive Detection of Acetylcholine in Protic Media: Artificial-Signaling Acetylcholine Receptors. *J. Am. Chem. Soc.* **1994**, *116*, 5517–5518.

17 a) Tan, S.-D.; Chen, W.-H.; Satake, A.; Wang, B.; Xu Z.-L.; Kobuke, Y. Tetracyanoresorcin[4]arene as a pH dependent artificial acetylcholine receptor. Org. Biomol. Chem., 2004, 2, 2719–2721. b) Koh, K. N.; Araki, K.; Ikeda, A.; Otsuka H.; Shinkai, S. Reinvestigation of Calixarene-Based Artificial-Signaling Acetylcholine Receptors Useful in Neutral Aqueous (Water/Methanol) Solution. J. *Am. Chem. Soc.* **1996,** *118*, 755–758.

18 Liu, Y.; Perez, L.; Mettry, M.; Gill, A. D.; Byers, S. R.; Easley, C. J.; Bardeen, C. J.; Zhong, W.; Hooley, R. J. Site selective reading of epigenetic markers by a dual-mode synthetic receptor array. *Chem. Sci.* **2017**, *8*, 3960-3970.

19 Korbakov, N.; Timmerman, P.; Lidich, N.; Urbach, B.; Sa'ar, A.; Yitzchaik, S. Acetylcholine Detection at Micromolar Concentrations with the Use of an Artificial Receptor-Based Fluorescence Switch. *Langmuir* **2008**, *24*, 2580–2587.

20 a) Dumartin, M.-L.; Givelet, C.; Meyrand, P.; Bibal B.; Gosse, I. A fluorescent cyclotriveratrylene: synthesis, emission properties and acetylcholine recognition in water. *Org. Biomol. Chem.* 2009, 7, 2725–2728. b) Erieau-Peyrard, L.; Coiffier, C.; Bordat, P.; Bégué, D.; Chierici, S.; Pinet, S.; Gosse, I.; Barailleb I.; Brown, R. Selective, direct detection of acetylcholine in PBS solution, with self-assembled fluorescent nano-particles: experiment and modelling. *Phys. Chem. Chem. Phys.* **2015**, *17*, 4168-4174.

21 Schneider, H.-J.; Güttes D.; Schneider, U. A Macrobicyclic Polyphenoxide as Receptor Analogue for Choline and Related Ammonium Compounds. *Angew. Chem. Int. Ed. Engl.* **1986**, *25*, 647–649.

22 Jia, C.; Zuo, W.; Yang, D.; Chen, Y.; Cao, L.; Custelcean, R.; Hostaš, J.; Hobza, P.; Glaser, R.; Wang, Y.-Y.; Yang X.-J.; Wu B. Selective binding of choline by a phosphate-coordination-based triple helicate featuring an aromatic box. *Nat. Commun.* **2017**, *8*, 938.

23 Hooley, R. J.; Van Anda H.; Rebek, J. Extraction of Hydrophobic Species into a Water-Soluble Synthetic Receptor. *J. Am. Chem. Soc.* **2007**, *129*, 13464–13473.

24 a) Ballester, P.; Shivanyuk, A.; Far A. R.; Rebek, J. A Synthetic Receptor for Choline and Carnitine *J. Am. Chem. Soc.* **2002**, *124*, 14014–14016. b) Ballester P.; Sarmentero, M. A. Hybrid Cavitand−Resorcin[4]arene Receptor for the Selective Binding of Choline and Related Compounds in Protic Media. *Org. Lett.* **2006**, *8,* 3477-3480.

25 Guo, D.-S.; Uzunova, V. D.; Su, X.; Liu Y.; Nau, W. M. Operational calixarene-based fluorescent sensing systems for choline and acetylcholine and their application to enzymatic reactions. *Chem. Sci.* **2011**, *2*, 1722–1734.

26 a) Hof, F.; Trembleau, L.; Ullrich E. C.; Rebek J. Acetylcholine Recognition by a Deep, Biomimetic Pocket. *Angew. Chem. Int. Ed.* **2003**, *42*, 3150–3153. b) Whiting A. L.; Hof, F. Binding trimethyllysine and other cationic guests in water with a series of indole-derived hosts: large differences in affinity from subtle changes in structure. *Org. Biomol. Chem.* **2012**, *10*, 6885–6892.

27 Garel, L.; Lozach, B.; Dutasta, J.-P.; Collet, A. Remarkable effect of the receptor size in the binding of acetylcholine and related ammonium ions to water-soluble cryptophanes. *J. Am. Chem. Soc.* **1993**, *115*, 11652–11653.

28 Peyrard, L.; Chierici, S.; Pinet, S.; Batat, P.; Jonusauskas, G.; Pinaud, N.; Meyrand P.; Gosse, I. C_3-triiodocyclotriveratrylene as a key intermediate to fluorescent probes: application to selective choline recognition. *Org. Biomol. Chem.* **2011**, *9*, 8489-8494.

29 Abdoul-Carime, H.; Farizon, B.; Farizon, M.; Mulatier, J.-C.; Dutasta J.-P.; Chermette, H. Solution vs. gas phase relative stability of the choline/acetylcholine cavitand complexes. P*hys. Chem. Chem. Phys.* **2015**, *17*, 4448–4457.

30 Bakirci H.; Nau, W. Fluorescence Regeneration as a Signaling Principle for Choline and Carnitine Binding: A Refined

Supramolecular Sensor System Based on a Fluorescent Azoalkane. A*dv. Funct. Mater.* **2006**, *16*, 237–242.

31 Zhang, D.; Martinez A.; Dutasta, J.-P. Emergence of Hemicryptophanes: From Synthesis to Applications for Recognition, Molecular Machines, and Supramolecular Catalysis. *Chem. Rev.* **2017**, *117*, 4900–4942.

32 Long, A.; Fantozzi, N.; Pinet, S.; Genin, E.; Pétuya, R.; Bégué, D.; Robert, V.; Dutasta, J.-P.; Gosse, I.; Martinez, A. Selective recognition of acetylcholine over choline by a fluorescent cage. *Org. Biomol. Chem.* **2019**, *17*, 5253-5257 .

33 Chatelet, B.; Payet, E.; Perraud, O.; Dimitrov-Raytchev, P.; Chapellet, L.-L.; Dufaud, V.; Martinez A.; Dutasta, J.-P. Shorter and Modular Synthesis of Hemicryptophane-tren Derivatives. *Org. Lett.* **2011**, *13*, 3706–3709.

34 Long, A.; Perraud, O.; Albalat, M.; Robert, V.; Dutasta J.-P.; Martinez, A. Helical Chirality Induces a Substrate-Selectivity Switch in Carbohydrates Recognitions. *J. Org. Chem.* **2018**, *83*, 6301–6306.

35 Hibbert D. B.; Thordarson, P. The death of the Job plot, transparency, open science and online tools, uncertainty estimation methods and other developments in supramolecular chemistry data analysis. *Chem. Commun.* **2016**, *52*, 12792–12805.

36 Perraud, O.; Robert, V.; Martinez A.; Dutasta, J.-P. A Designed Cavity for Zwitterionic Species: Selective Recognition of Taurine in Aqueous Media. *Chem. Eur. J.*, **2011**, *17*, 13405–13408.

37 Frisch, M. J.; Trucks, G. W.; Schlegel, H. B.; Scuseria, G. E.; Robb, M. A.; Cheeseman, J. R.; Scalmani, G.; Barone, V.; Mennucci, B.; Petersson, G. A.; Nakatsuji, H.; Caricato, M.; Li, X.; Hratchian, H. P.; Izmaylov, A. F.; Bloino, J.; Zheng, G.; Sonnenberg, J. L.; Hada, M.; Ehara, M.; Toyota, K.; Fukuda, R.; Hasegawa, J.; Ishida, M.; Nakajima, T.; Honda, Y.; Kitao, O.; Nakai, H.; Vreven, T.; Montgomery, J. A., Jr.; Peralta, J. E.; Ogliaro, F.; Bearpark, M.; Heyd, J. J.; Brothers, E.; Kudin, K. N.; Staroverov, V. N.; Keith, T.; Kobayashi, R.; Normand, J.; Raghavachari, K.; Rendell, A.; Burant, J. C.; Iyengar, S. S.; Tomasi, J.; Cossi, M.; Rega, N.; Millam, J. M.; Klene, M.; Knox, J. E.; Cross, J. B.; Bakken, V.; Adamo, C.; Jaramillo, J.; Gomperts, R.; Stratmann, R. E.; Yazyev, O.; Austin, A. J.; Cammi, R.; Pomelli, C.; Ochterski, J. W.; Martin, R. L.; Morokuma, K.; Zakrzewski, V. G.; Voth, G. A.; Salvador, P.; Dannenberg, J. J.; Dapprich, S.; Daniels, A. D.; Farkas, O.; Foresman, J. B.; Ortiz, J. V.; Cioslowski, J.; Fox, D. J. Gaussian, Inc.: Wallingford, CT.

SYNOPSIS TOC. The selective recognition of acetylcholine over choline was achieved with the synthesis of new hemicryptophane hosts presenting improved fluorescence properties.

Insert Table of Contents artwork here

- Red-shifted emission
- Improved quantum yield
- Acetylcholine/choline selectivity
- High binding constant (>10^4)